



A full-spectrum synergetic management strategy for passive cooling of solar cells

Kegui Lu, Bin Zhao^{**}, Chengfeng Xu, Xiansheng Li, Gang Pei^{*}

Department of Thermal Science and Energy Engineering, University of Science and Technology of China, Hefei, 230027, China

ARTICLE INFO

Keywords:

Solar cells
Radiative cooling
Selective-spectrum
Passive cooling
Solar splitting

ABSTRACT

Cooling solar cells towards ambient temperature is essential for photovoltaic conversion since the elevated temperature has significant adverse consequences on the efficiency and reliability of solar cells. Here, a full-spectrum synergetic management strategy that is developed by enhancing radiative cooling of solar cells in the Mid-Infrared and selectively reducing the cell's sub-band-gap (sub-BG) absorption in solar wavelengths, is proposed to cool solar cells. To experimentally demonstrate the feasibility of the concept, a cooling system demo is developed by integrating a spectral-selective mirror (SS-Mirror) to selective block sub-BG photons and a radiative cooler for heat radiation. A temperature drop of 7.1 °C and an open-circuit voltage enhancement of 38 mV are observed under a solar simulator with 1 sun input. Moreover, a model is applied to capture the cooling performance of the proposed idea of solar cell cooling under various conditions, including for concentration photovoltaic cases. This study proposes a full-spectrum synergetic management method to passively cool solar cells and makes an experimental validation, providing a new pathway to cool solar cells.

1. Introduction

Photovoltaic (PV) conversion can convert solar energy into clean electricity directly and has attracted much attention since it has been widely recognized as one of the promising clean solutions to the world's energy problems [1–4]. At present, the efficiency of commercial solar cells is in the region of 20–30%, while the solar absorption of solar cells is generally over 0.9, which means the majority of absorbed solar energy is converted into heat and then improves the operating temperature of solar cells. However, the efficiency [5–7] of solar cells degenerates at high temperatures as well as the reliability [8]. For commonly used monocrystalline silicon solar cells, the theoretical upper limit for power conversion efficiency is about 33.7% [9], while the solar absorption of the cell reaches more than 0.9 due to the synergistic effect of intrinsic absorption and anti-reflection design, resulting in nearly 600 W·m⁻² heat flux will be generated in solar cells under the AM 1.5 solar spectrum. The waste heat improves the cell's temperature to 30–50 °C above ambient temperature [10–12] and decreases its relative efficiency by approximately 13.5%–22.5% [13]. Therefore, cooling solar cells is critical for PV conversion.

According to the heat transfer theory, three heat transfer modes that

include heat conduction, heat convection, and heat radiation can be potentially used in the cooling of solar cells. Most of the previously published works use heat convective or conductive modes to cool solar cells, including air cooling [14], water cooling [15], microchannel [16], and phase change materials (PCMs) [17,18], which require additional energy consumption and extra complex heat exchange/storage structures. For example, the structure of PCMs-based solar panels is comparatively complex, and continuous cooling is not achieved since the solar heating of the panel is greater than the latent heat of the PCMs. For active water cooling, additional components (e.g., copper tubes and water pump) and extra electrical energy are required. In recent years, radiative cooling of solar cells based on heat radiation mode has been proposed and increase much interest [19–26], which is a passive cooling method without extra energy input. The fundamental principle is to place a radiative cooler that is solar transparent but strongly emissive over mid-infrared wavelengths, especially within the atmosphere transparency window from 8 to 13 μm, on top of solar cells to enhance heat dissipation. The radiative cooler does not degrade the optical performance of solar cells but does generate a significant cooling effect for solar cells by mainly emitting waste heat to outer space (~3 K). In 2014, Zhu et al. [27] proposed the concept of radiative cooling of solar cells

* Corresponding author.

** Corresponding author.

E-mail addresses: zb630@ustc.edu.cn (B. Zhao), peigang@ustc.edu.cn (G. Pei).

and predicted that a temperature reduction of 18.3 K can be obtained using a periodic pyramid micro-structure-based silica cooler. Besides, an experimental demonstration is also conducted to reveal that the silicon solar cell can be radiatively cooled by 13 K after using a silica photonic cooler. These findings have aroused much attention for radiative cooling of solar cells [28–33]. Zhou et al. theoretically improved the thermal emissivity of low-iron soda-lime glass by an additional multilayer [34] or patterned surface [35] to enhance the radiative cooling capacity of the glass cover. In addition to silicon-based solar cells and flat plate solar PV conversion (i.e., no solar concentration), radiative cooling methods can be also used to cool different types of solar cells (e.g., CIGS [36] and GaAs [37,38] solar cells) and various PV applications (e.g., CPV [38–40], thermal PV (TPV) [35], and outer space PV applications [41]).

Although radiative cooling can provide sustainable passive cooling for solar cells, the cooling performance can be improved when combining the solar splitting method. Specifically, if solar cells can effectively reflect sub-band-gap (sub-BG) photons, the operating temperature can be further reduced. Sun et al. [36,42] found that the solar cell can be further cooled by approximately 6 °C after reflecting sub-BG photons. The reason for this scenario is that only above-band-gap (above-BG) photons can stimulate the generation of electron-hole pairs, while the sub-BG photons produce thermal effects. Li et al. [43] proposed a photonic cooler design that can simultaneously achieve radiative cooling of solar cells and selectively reduce the cell's sub-BG absorption. Simulation results show that a solar panel can be cooled by over 5.7 °C after using the photonic cooler. Zhao et al. [44] also designed a similar 2D photonic cooler to cool solar cells. The combined optical, thermal, and electrical simulation shows that the temperature of solar cells can be reduced by approximately 8 °C. Analogously, An et al. [45] proposed a photonic radiative cooler with near-ideal spectral selectivity from the sunlight to the infrared band for thermal management of solar cells. It is demonstrated that the absolute efficiency of the solar cells is increased by ~0.43% and a reduction in the solar cells operating temperature by ~10.16 °C can be obtained. Although the above-mentioned cooling idea of solar cells is a kind of combination of spectral splitting cooling and radiative cooling, the reported works are all simulations that involve thermal performance prediction and optical filter design. The main reason for this scenario is that a single optical filter is used for both spectral splitting and radiative cooling, which is currently difficult for structure design and fabrication. Thus, the experimental demonstration of this full-spectrum management for cell cooling based on an appropriate implementation solution is emergently required.

Herein, we propose a full-spectrum synergetic management (FSSM) strategy to cool solar cells, which combines radiative cooling and spectral splitting to enhance radiative heat dissipation and reduce the waste heat generated by the absorption of sub-BG photons. An experimental demonstration for the proposed FSSM strategy is conducted. A cooling system demo is designed by integrating an individual spectral-selective mirror (SS-Mirror) and an individual radiative cooler. The

SS-Mirror is applied to selective block sub-BG photons and the radiative cooler is used for heat radiation dissipation. The cooling of solar cells demonstration is conducted under 1 sun condition using a solar simulator and the temperature and open-circuit voltage of the solar cell are monitored. Moreover, a mathematical model is developed to predict the cooling performance of the proposed idea for solar cells under various conditions, including for various concentration ratios.

2. Results and discussion

2.1. The full-spectrum synergetic management strategy

The main principle of the proposed full-spectrum synergetic management (FSSM) strategy is that an SS-Mirror and a radiative cooler are separately applied in the cell cooling system to block the sub-BG photons and enhance thermal emission (Fig. 1a), which is quite different from the published strategy that uses a single optical film to simultaneously regulate spectral behavior for sunlight and mid-infrared thermal radiation. For crystalline silicon cells, the spectral selective requirements of the SS-Mirror and radiative cooler are shown in Fig. 1b. The SS-Mirror needs to have high reflectivity within the wavelength region of 0.3–1.1 μm since the bandgap of the silicon cell is around 1.1 eV, ensuring that above-BG photons can be reflected to solar cells for electricity generation. Besides, low reflectivity in the wavelength region of over 1.1 μm is also desired for SS-Mirror to maximally block the sub-BG photons. Moreover, the radiative cooler needs to have high solar reflection and strong thermal emission so that the cooler can act as an efficient radiative heat emitter.

2.2. SS-mirror and radiative cooler

According to the spectral requirements, an SS-Mirror and a radiative cooler are prepared for the cooling system demo. The SS-Mirror (Fig. 2a) is a 3 M ESR film, which is widely used in previously published papers on the topic of radiative cooling [19,46]. The 3 M ESR film is composed of multilayer polymer layers and the radiative cooler with excellent solar reflection and strong infrared emission is a metamaterial that contains micrometer-sized silica spheres randomly distributed in the matrix material of polymethylpentene and coupled with a highly reflective silver layer on the back [47]. To characterize the optical properties of the SS-Mirror and radiative cooler, the spectral reflectivity and transmissivity of the planar samples are measured and the emissivity values are then obtained using the law of energy balance and Kirchhoff's law. As shown in Fig. 2b, the SS-Mirror exhibits strong reflectivity in the region of 0.38–1.1 μm with a weighted reflectivity of nearly 0.95 and has great transmissivity for sub-BG photons with a weighted transmissivity of nearly 0.83, showing obvious spectrally selective reaction for sunlight. Moreover, the specular reflectivity of the SS-Mirror with different incident angles is also evaluated and the results show that the specular reflectivity of the SS-Mirror is not sensitive to the angle (Fig. 2c), which

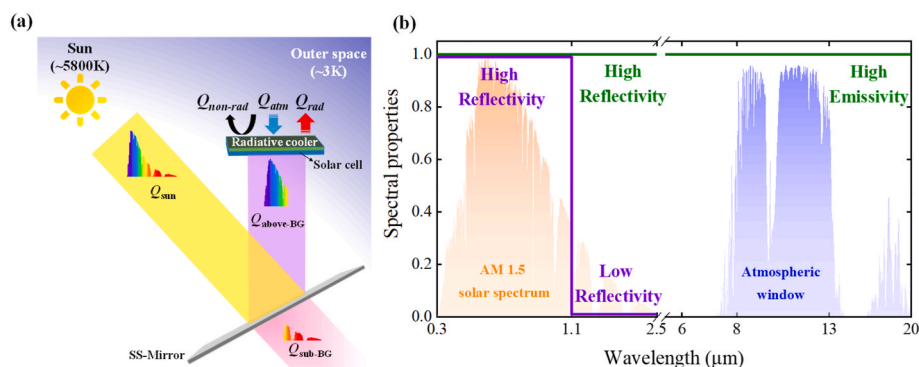


Fig. 1. (a) Schematic of the FSSM strategy. (b) Spectral requirements of the SS-Mirror and radiative cooler.

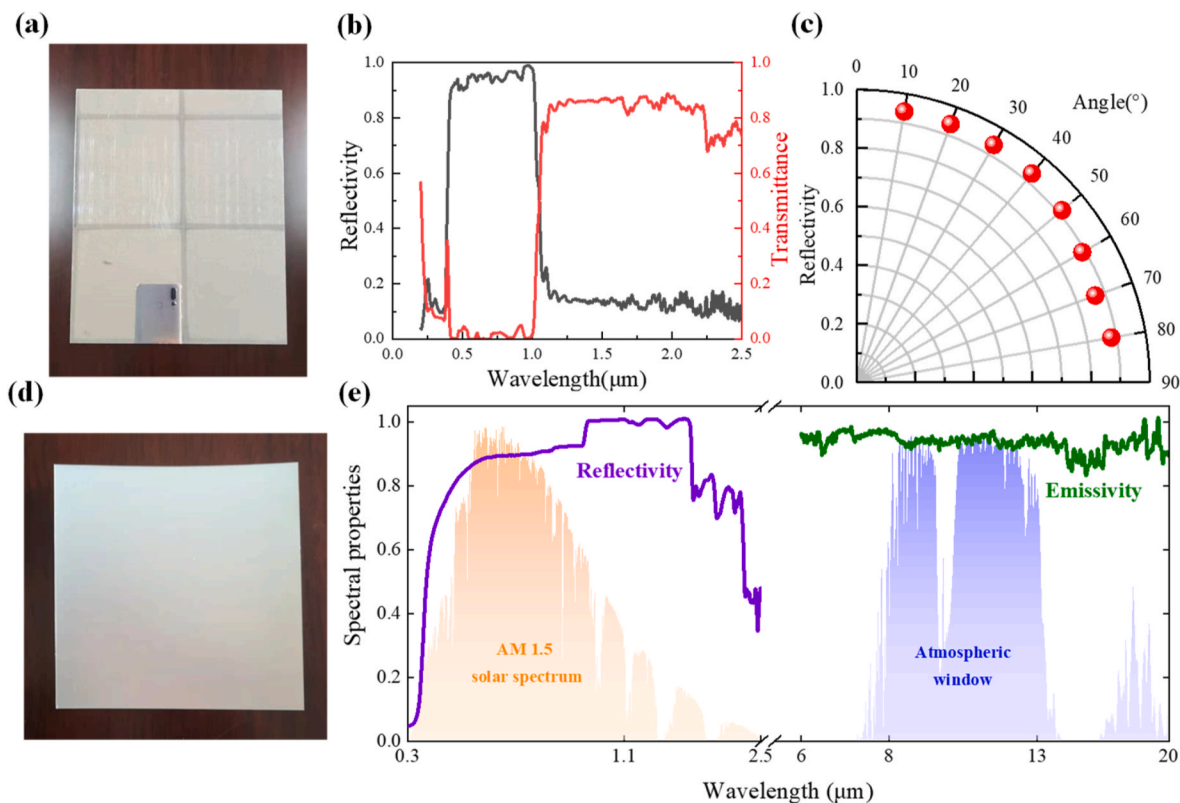


Fig. 2. (a) The photo of the SSM mirror. (b) Measured reflectivity and transmissivity of the SS-Mirror in the solar band. (c) Measured specular reflectivity of the SS-Mirror with different incident angles. (d) The photo of the radiative cooler. (e) Measured reflectivity of the radiative cooler in the solar band and thermal emissivity of the radiative cooler in the mid-infrared wavelength band.

is a great feature for the design of the cooling system. For the radiative cooler (Fig. 2d–e), it has a strong solar reflection in the solar band to prevent the solar heating on the cooler and it behaves like a blackbody in the mid-infrared wavelength band to radiatively dissipate heat into outer space.

2.3. Experimental demonstration

A demo of the cell cooling system based on the FSSM strategy is built to investigate the cooling performance of the proposed strategy for silicon solar cells. The schematic and diagram of the system design are

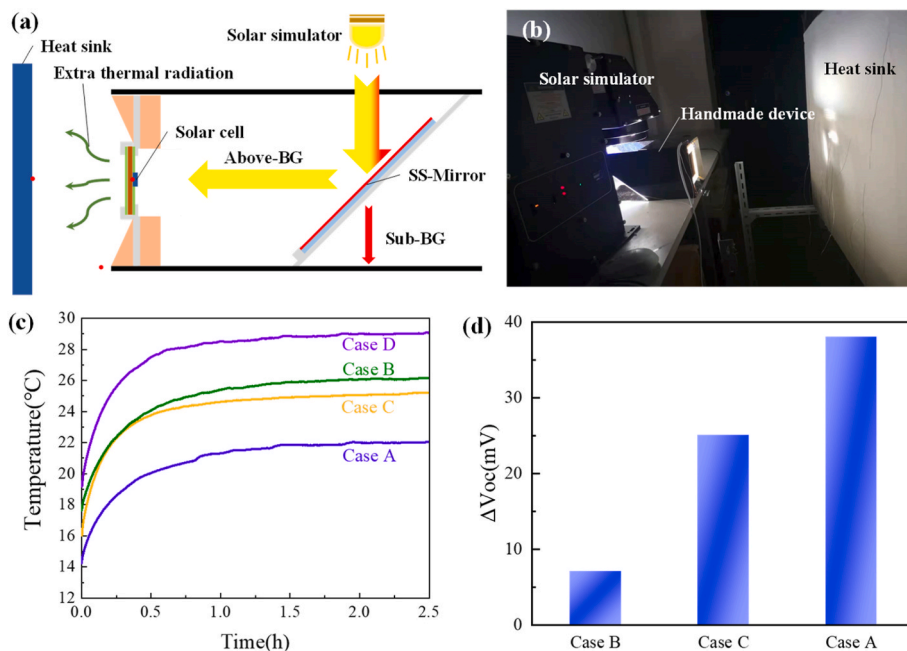


Fig. 3. (a) Schematic of cooling system demo. (b) Photo of the cooling system demo. (c) Measured transient temperature of the solar cells for Case A, B, C, and D. (d) Measured V_{oc} difference of solar cells in different cases.

shown in Fig. 3a–b, the SS-Mirror is fixed with an inclination angle of 45° to selectively reflect the parallel light generated by the solar simulator for the vertical direction. A solar cell assembly is fixed at the center of the chamber to receive the above-BG photons reflected by the SS-Mirror. The surfaces of the chamber (Fig. S1) are made of black PMMA to avoid interference from external light and scattered light. The solar cell assembly (Fig. S2) is a multi-layer structure. A silicon solar cell is fixed at a copper plate using thermally conductive grease and radiative coolers are attached to the backside of the copper for heat dissipation. Besides, a reflective layer is also attached to the front side of the copper to minimize the solar heating of the copper plate. To simulate the properties of the cold sky, an aluminum box (0.8 m × 0.8 m × 0.1 m) with dry ice filled in is used as a heat sink and similar assumptions and experiments have been already reported [19,48]. The box surface is covered with a layer of black paint and its emissivity is shown in Fig. S3. The temperature of the chamber surface is approximately 208 K (Fig. S4). To keep the heat sink at a low temperature, dry ice is continuously added to the aluminum box during the whole experiment process with an interval period of 20 min. At the steady-state, the open-circuit voltage (V_{oc}) of the solar cell is measured by the PVIV test station (PVIV-10A-I-AMP, Newport). During the experiment, T-type thermocouples are applied to monitor the temperature of the solar cell.

Four different conditions, including Case A, B, C, and D, are considered in the experiment. Case A represents the proposed FSSM strategy since SS-Mirror and radiative cooler are both applied. Case B only applies an SS-Mirror, which means the copper surface of the solar assembly is directly exposed to the heat sink. Case C uses a Normal-Mirror that has a high solar reflection in the whole solar band and a radiative cooler. The reflectivity of the copper and Normal-Mirror are shown in Fig. S5, with the solar absorptivity of the silicon cell plotted as a reference. Case D is a reference. Fig. 3c shows that the temperature of the solar cell for Case A is always the lowest among the four cases. At a steady-state, the temperature of the solar cell for Case A is about 7.1 °C lower than that for Case D, which demonstrates the passive cooling performance of the proposed FSSM strategy. Moreover, the temperature values of the solar cell for Case B and Case C are also lower than that for Case D, which means radiative cooling and selective harvesting of photons are also alternative cooling methods for solar cells. It is noted that the steady-state temperature of solar cells still varies at a very slow rate and this is due to the fluctuation of ambient temperature in the room and the continuous formation of frost on the surface of the heat sink. Besides the cell temperature, the V_{oc} of the solar cell is also measured for comparison, and results (Fig. 3d) clearly show that the V_{oc} of the solar cell for Case A is the highest among the concerned four cases. As expected, the change of V_{oc} is opposite to the variation of operating temperature among the four cases. Specifically, the V_{oc} of the solar cell for Case A is 38 mV higher than that of the reference case, corresponding to an improvement of 1.7%. Besides, the temperature of the bare cell under direct sunlight is also tested, and the result shows that the temperature of the cell is 12.8 °C higher than that under case A, which also causes a reduction of V_{oc} . Both the benefit of temperature reduction and V_{oc} improvement demonstrate the passive cooling effect of the proposed FSSM strategy.

Notably, although the FSSM strategy brings advantages to solar cells in terms of V_{oc} and operating temperature, the effect of the optical efficiency should be further considered in future work. The use of the SS-Mirror may reduce the effective reflection for above-BG photons because the spectral properties of the SS-Mirror are not good enough, which corresponds to the efficiency reduction. So, spectral optimization of the SS-Mirror for effective spectral splitting is also an important topic for photovoltaic conversion.

A brief comparison among existing passive cooling methods for solar cells is conducted and is shown in Table 1. PCMs have a good cooling effect, but the structure is comparatively complex and the cooling time is restricted due to the limited cooling capacity of PCMs. Besides, the use of PCMs will enlarge the quality of the system and bring the additional

Table 1

Summary of the experimental solar cell passive cooling methods. (Notes: RC means radiative cooling; SS means spectral splitting).

Authors	Method	Type of cell	Temperature reduction	Notes
Hasan et al. [51]	PCMs	Poly-Si cell	18 °C	Outdoor experiment
Nada et al. [52]	PCMs	Poly-Si cell	~8.1 °C	Outdoor experiment
Oztop et al. [53]	Heat fins	Poly-Si cell	<1 °C	Outdoor experiment
Zhu et al. [23]	RC	p-doped silicon	5.2 °C	Without cover
Zhao et al. [26]	RC	Si cell	13 °C	With cover
Wang et al. [54]	RC	Si cell	3.6 °C	With cover
Gao et al. [55]	RC	Si cell	4 °C	With cover
This work	RC & SS	Si cell	17 °C	Within insulation box
			7.1 °C	Without cover

problem of heat storage/release process [49,50]. Using heat sinks for solar cells is also a passive cooling method, but the cooling effect is limited, and additional heat sinks are required. Radiative cooling is an emerging passive cooling method for solar cells, which requires no energy input and additional structures, but the cooling performance can be further improved after coupling the appropriate management of the solar spectrum and this is what we do in this work.

2.4. Performance prediction

To further explore the cooling effect of the proposed strategy for solar cells under different situations, a simulation study based on a steady-state condition is conducted. The energy balance process of the solar cell is presented in Fig. 4a and the cell is related to sunlight, atmosphere, and ambient air. According to the first law of thermodynamics, the governing equation of the cell can be expressed as:

$$P_{rad}(T_{cell}) - P_{sun} - P_{atm}(T_{amb}) + P_{non-rad}(T_{cell}, T_{amb}) = 0 \quad (1)$$

where T_{cell} is cell temperature and T_{amb} is ambient temperature. The radiative heat flux of the solar cell $P_{rad}(T_{cell})$ is expressed as:

$$P_{rad}(T_{cell}) = 2\pi \int_0^\pi \int_0^{\frac{\pi}{2}} I_{BB}(\lambda, T_{cell}) \epsilon_{cell}(\lambda, \theta) \cos \theta \sin \theta d\theta d\lambda \quad (2)$$

where $I_{BB}(\lambda, T_{cell})$ is the spectral radiance density of a blackbody at T_{cell} , $\epsilon_{cell}(\lambda, \theta)$ is the spectral-angular emissivity of the solar cell. The absorbed solar flux P_{sun} can be expressed as:

$$P_{sun} = G \alpha_{cell} \quad (3)$$

where G is the total solar power flux and α_{cell} is the AM 1.5 weighted solar absorptivity of the solar cell. The absorbed atmospheric heat flux $P_{atm}(T_{amb})$ can be expressed as:

$$P_{atm}(T_{amb}) = 2\pi \int_0^\pi \int_0^{\frac{\pi}{2}} I_{BB}(\lambda, T_{amb}) \epsilon_{cell}(\lambda, \theta) \epsilon_{atm}(\lambda, \theta) \cos \theta \sin \theta d\theta d\lambda \quad (4)$$

where $\epsilon_{atm}(\lambda, \theta) = 1 - \tau(\lambda, 0)^{1/\cos \theta}$ [56] is an estimate of the spectral angular emissivity of the atmosphere and $\tau(\lambda, 0)$ is the transmittance of the atmosphere at the vertical direction. The non-radiative heat flux of the solar cell $P_{non-rad}(T_{cell}, T_{amb})$ is can be described using an overall heat transfer coefficient h_c :

$$P_{non-rad}(T_{cell}, T_{amb}) = h_c (T_{cell} - T_{amb}) \quad (5)$$

During simulation, the spectral atmospheric transmittance in mid-latitude winter is used and obtained from the MODTRAN [57]. The ambient temperature is set as 293 K and the overall heat transfer

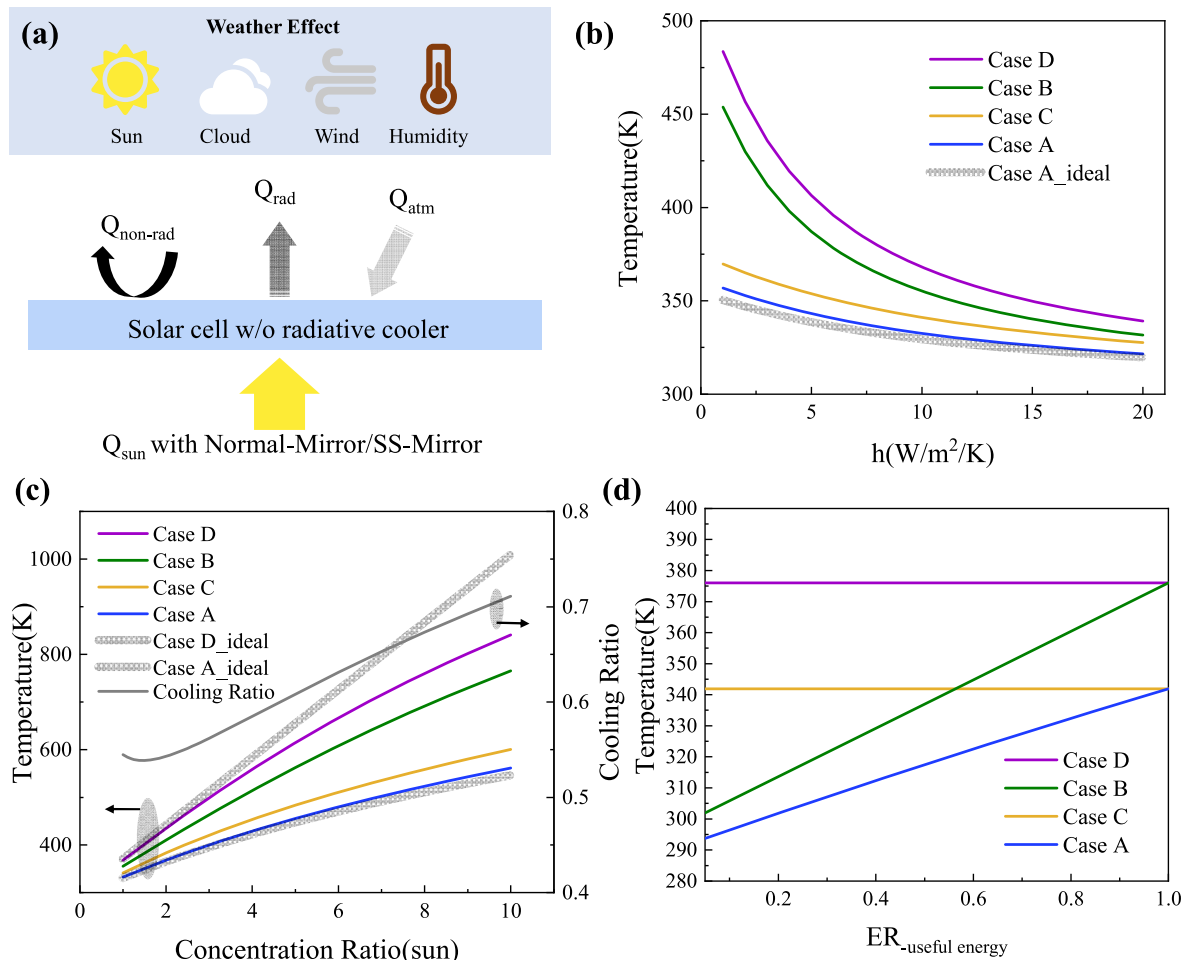


Fig. 4. (a) Energy balance process of the solar cell. (b) The temperature of the solar cell under different h_c values. (c) The temperature of the solar cell under different concentration ratios. (d) The temperature of the solar cell under different $ER_{\text{useful energy}}$.

coefficient is set to be $10 \text{ W m}^{-2} \text{ K}^{-1}$ ($\sim 2.4 \text{ m/s}$ wind speed) [27]. The spectral properties used in the simulation are shown in Fig. S5. Besides, 1000 W m^{-2} solar irradiance with AM 1.5 solar spectrum is also selected as input. Fig. 4b shows the steady-state temperature of solar cells under different cases with different h_c values. It can be found that the temperature of the solar cell under case A is always the lowest, which is consistent with the experimental results presented in Fig. 3c, indicating that the proposed FSSM strategy has the best cooling effect for solar cells. For example, the temperature of the solar cell under case A is 24°C lower than that under case D when h_c equals $10 \text{ W m}^{-2} \text{ K}^{-1}$ and this temperature difference enlarges to 57°C when h_c decreases to $3 \text{ W m}^{-2} \text{ K}^{-1}$ (nearly windless). Besides, when h_c increases, the temperature of the solar cell under different cases decreases due to the enhancement of convection heat dissipation. Notably, the temperature of the solar cell under the ideal case (i.e., Case A_ideal) with perfect spectral properties of SS-Mirror and radiative cooler is also considered and the temperature curve is very close to that of Case A, showing the great cooling potential of the current SS-Mirror and radiative cooler. To analyze the potential of the proposed strategy, an annual simulation analysis with typical meteorological year data at different locations (i.e., Hefei, China and Jiuquan, China) is conducted (Fig. S7). In the two places, the solar cell's operating temperature under Case A is lower than that of Case D. Specifically, the mean temperature difference in Hefei, China is about 5.1 K , and the cooling performance in Jiuquan, China is better than that in Hefei with a mean temperature difference of 8.1 K , which corresponds to about 3.6% relative efficiency promotion for silicon cell in terms of the temperature effect.

The effect of the concentration ratio of solar cells is also evaluated due to the potential application of concentration PV (CPV). As shown in Fig. 4c, the temperature of the solar cell under Case A is still the lowest. Besides, the temperature of the solar cell increases almost linearly with the increased concentration ratio, but the temperature increase rate of the cell with enhanced radiative cooling is obviously lower than others. This scenario is caused by the reason that the radiative heat power of the radiative cooler is proportional to the fourth power of the temperature so that the cooling effect of radiative cooling is highlighted at high temperatures. To further show the cooling performance of the proposed FSSM strategy for solar cells in CPV applications, a cooling ratio (CR) is defined and applied:

$$CR = \frac{T_n - T_{FSSM}}{T_n - T_{amb}} \quad (6)$$

where T_n is the temperature of the solar cell under Normal-Mirror without radiative cooling completely in mid-infrared (i.e., Case D_ideal) and T_{FSSM} denotes the temperature of solar cell under proposed FSSM with ideal spectral properties (i.e., Case A_ideal). Ambient temperature T_{amb} is set as 293.15 K . CR increases almost constantly with the increase of concentration ratio and reaches up to over 0.7 at 10 suns, which is great than those for Case B and Case C, showing the proposed FSSM is a good cooling method candidate for CPV applications at high concentration ratio.

The above investigations are conducted based on crystalline silicon solar cells. Here, the proposed FSSM cooling strategy is extended to various solar cells with different band-gap properties. We define a

parameter ER_useful energy to describe the proportion of energy of photons that can generate electricity to the energy of total photons of incident light. Fig. 4d shows the temperature of the solar cell under Case A and Case B are sensitive to ER_useful energy since selective utilization of sunlight is included, while the cell temperature under Case C is stable. It can be also found that the temperature of the solar cell under Case B and Case C is the same at critical ER_useful energy (~ 0.56). When ER_useful energy enlarges than the critical point, the cooling effect of radiative cooling becomes more efficient, while selective utilization of sunlight is more useful at low ER_useful energy. Importantly, the cell temperature under Case A is always the lowest, demonstrating the cooling potential of the proposed FSSM.

3. Experimental procedures

3.1. Material characterizations

The spectral reflectivity and transmissivity of the sample in the wavelength region of 0.3–2.5 μm are measured by a UV–Vis–NIR spectrometer (SolidSpec-3700 DUV, Shimadzu) equipped with a Teflon-coated integrating sphere. The angular-specular reflectivity of the sample is measured by a variable angle measuring attachment for SolidSpec-3700 DUV. Besides, the spectral reflectivity of the sample in 2.5–20 μm is measured by a Fourier transform infrared spectrometer (Nicolet iS 50, Thermo Scientific) equipped with a gold-coated integrating sphere.

3.2. Cooling performance measurement

A solar simulator (Oriel Sol3A Class AAA, Newport) is used as the simulated sunlight. The room temperature and humidity are controlled by an air-conditioner throughout the whole experiment process. The positions of temperature measurement are marked as red points in Fig. 3 (a) by T-type thermocouples with an accuracy of ± 0.5 $^{\circ}\text{C}$. The data of temperature and humidity are all recorded using a data acquisition instrument (LR8450, HIOKI). To keep the heat sink at a low temperature, dry ice is continuously added to the aluminum box during the whole experiment process with an interval period of 20 min. At the steady-state, the Voc of the solar cell is measured by the PVIV test station (PVIV-10A-I-AMP, Newport).

4. Conclusion

This paper proposes a full-spectrum synergetic management (FSSM) strategy to cool solar cells passively. A cooling system demo, which means full-spectrum heat management is experimentally achieved firstly, is developed by integrating an SS-Mirror to selective block sub-BG photons and a radiative cooler for radiative cooling of solar cells. Experiment demonstration and numerical prediction are conducted to capture the cooling performance of the solar cell. The results are summarized as follows:

- (1) The proposed FSSM strategy can passively cool solar cells. A temperature drop of 7.1 $^{\circ}\text{C}$ and an open-circuit voltage enhancement of 38 mV are obtained under a solar simulator with 1 sun input.
- (2) The cooling effect of the proposed FSSM strategy is better than that of the methods that only enhance radiative cooling and selectively harvest photons.
- (3) The proposed FSSM strategy has the potential to effectively cool CPV. For 10 suns concentration, the temperature increment of the solar cell in CPV condition can be reduced by up to over 70%.
- (4) The proposed FSSM can passively cool solar cells for various conditions, including the existence of convection heat transfer, different concentration ratios, and various cells with different bandgaps.

In summary, this work proposes an FSSM strategy to passively cool solar cells without extra power input and makes an experimental demonstration, providing a new pathway to cool solar cells, especially for solar cells with high bandgap and CPV applications.

CRediT authorship contribution statement

Kegui Lu: Writing – review & editing, Writing – original draft, Software, Methodology, Formal analysis. **Bin Zhao:** Writing – review & editing, Supervision, Project administration, Methodology, Funding acquisition. **Chengfeng Xu:** Writing – review & editing, Formal analysis. **Xiansheng Li:** Writing – review & editing, Funding acquisition. **Gang Pei:** Writing – review & editing, Supervision, Project administration, Methodology, Funding acquisition.

Declaration of competing interest

The authors declare that they have no known competing financial interests or personal relationships that could have appeared to influence the work reported in this paper.

Data availability

Data will be made available on request.

Acknowledgments

This work was supported by the National Natural Science Foundation of China (52106276 and 52130601), Project funded by China Postdoctoral Science Foundation (2020TQ0307 and 2020M682033), the Fundamental Research Funds for the Central Universities (WK2090000028), and Research center for multi-energy complementation and conversion of USTC.

Appendix A. Supplementary data

Supplementary data to this article can be found online at <https://doi.org/10.1016/j.solmat.2022.111860>.

References

- [1] L. Zhu, L. Wang, C. Pan, L. Chen, F. Xue, B. Chen, L. Yang, L. Su, Z.L. Wang, Enhancing the efficiency of silicon-based solar cells by the piezo-phototronic effect, *ACS Nano* 11 (2017) 1894–1900.
- [2] M. Barbato, E. Artegiani, M. Bertoncello, M. Meneghini, N. Trivellin, E. Mantoan, A. Romeo, G. Mura, L. Ortolani, E. Zanoni, G. Meneghesso, CdTe solar cells: technology, operation and reliability, *J. Phys. Appl. Phys.* 54 (2021).
- [3] I. Etxebarria, J. Ajuria, R. Pacios, Solution-processable polymeric solar cells: a review on materials, strategies and cell architectures to overcome 10, *Org. Electron.* 19 (2015) 34–60.
- [4] R. Fornari, Optimal-growth conditions and main features of GaAs single-crystals for solar-cell technology - a review, *Sol. Energy Mater.* 11 (1985) 361–379.
- [5] P. Singh, N.M. Ravindra, Temperature dependence of solar cell performance—an analysis, *Sol. Energy Mater. Sol. Cell.* 101 (2012) 36–45.
- [6] M. Taguchi, E. Maruyama, M. Tanaka, Temperature dependence of amorphous/crystalline silicon heterojunction solar cells, *Jpn. J. Appl. Phys.* 47 (2008) 814–818.
- [7] M. Khalis, R. Masrou, G. Khrypunov, M. Kirichenko, D. Kudiy, M. Zazoui, Effects of temperature and concentration mono and polycrystalline silicon solar cells: extraction parameters, *J. Phys. Conf.* 758 (2016).
- [8] P. Espinet-González, C. Algora, N. Núñez, V. Orlando, M. Vázquez, J. Bautista, K. Araki, Temperature accelerated life test on commercial concentrator III-V triple-junction solar cells and reliability analysis as a function of the operating temperature, *Prog. Photovoltaics Res. Appl.* 23 (2015) 559–569.
- [9] L.C. Hirst, N.J. Ekins-Daukes, Fundamental losses in solar cells, *Prog. Photovoltaics Res. Appl.* 19 (2011) 286–293.
- [10] M.W. Davis, A.H. Fannoy, B.P. Dougherty, Prediction of building integrated photovoltaic cell temperatures, *J. Sol. Energy Eng.* 123 (2001) 200–210.
- [11] J.G. Ingersoll, Simplified calculation of solar-cell temperatures in terrestrial photovoltaic arrays, *J. Sol. Energy-T Asme* 108 (1986) 95–101.
- [12] A.D. Jones, C.P. Underwood, A thermal model for photovoltaic systems, *Sol. Energy* 70 (2001) 349–359.

- [13] E. Skoplaki, J.A. Palyvos, On the temperature dependence of photovoltaic module electrical performance: a review of efficiency/power correlations, *Sol. Energy* 83 (2009) 614–624.
- [14] H.G. Teo, P.S. Lee, M.N.A. Hawlader, An active cooling system for photovoltaic modules, *Appl. Energy* 90 (2012) 309–315.
- [15] H. Bahaidarah, A. Subhan, P. Gandhidasan, S. Rehman, Performance evaluation of a PV (photovoltaic) module by back surface water cooling for hot climatic conditions, *Energy* 59 (2013) 445–453.
- [16] K. Yang, C. Zuo, A novel multi-layer manifold microchannel cooling system for concentrating photovoltaic cells, *Energy Convers. Manag.* 89 (2015) 214–221.
- [17] M.J. Huang, P.C. Eames, B. Norton, Phase change materials for limiting temperature rise in building integrated photovoltaics, *Sol. Energy* 80 (2006) 1121–1130.
- [18] Z. Yu, D. Feng, Y. Feng, X. Zhang, Thermal conductivity and energy storage capacity enhancement and bottleneck of shape-stabilized phase change composites with graphene foam and carbon nanotubes, *Compos. Appl. Sci. Manuf.* 152 (2022).
- [19] D. Zhao, A. Aili, Y. Zhai, J. Lu, D. Kidd, G. Tan, X. Yin, R. Yang, Subambient cooling of water: toward real-world applications of daytime radiative cooling, *Joule* 3 (2019) 111–123.
- [20] T. Li, Y. Zhai, S.M. He, W.T. Gan, Z.Y. Wei, M. Heidarinejad, D. Dalgo, R.Y. Mi, X. P. Zhao, J.W. Song, J.Q. Dai, C.J. Chen, A. Aili, A. Vellore, A. Martini, R.G. Yang, J. Srebric, X.B. Yin, L.B. Hu, A radiative cooling structural material, *Science* 364 (2019) 760–763.
- [21] Z. Chen, L. Zhu, A. Raman, S. Fan, Radiative cooling to deep sub-freezing temperatures through a 24-h day-night cycle, *Nat. Commun.* 7 (2016), 13729.
- [22] D. Li, X. Liu, W. Li, Z. Lin, B. Zhu, Z. Li, J. Li, B. Li, S. Fan, J. Xie, J. Zhu, Scalable and hierarchically designed polymer film as a selective thermal emitter for high-performance all-day radiative cooling, *Nat. Nanotechnol.* 16 (2021) 153–158.
- [23] L. Zhu, A.P. Raman, S. Fan, Radiative cooling of solar absorbers using a visibly transparent photonic crystal thermal blackbody, *Proc. Natl. Acad. Sci. U. S. A.* 112 (2015) 12282–12287.
- [24] B. Zhao, M. Hu, X. Ao, N. Chen, G. Pei, Radiative cooling: a review of fundamentals, materials, applications, and prospects, *Appl. Energy* 236 (2019) 489–513.
- [25] X.B. Yin, R.G. Yang, G. Tan, S.H. Fan, Terrestrial radiative cooling: using the cold universe as a renewable and sustainable energy source, *Science* 370 (2020) 786–791.
- [26] B. Zhao, K. Lu, M. Hu, J. Liu, L. Wu, C. Xu, Q. Xuan, G. Pei, Radiative cooling of solar cells with micro-grating photonic cooler, *Renew. Energy* 191 (2022) 662–668.
- [27] L. Zhu, A. Raman, K.X. Wang, M.A. Anoma, S. Fan, Radiative cooling of solar cells, *Optica* 1 (2014).
- [28] I.M. Slauch, M.G. Deceglie, T.J. Silverman, V.E. Ferry, Spectrally selective mirrors with combined optical and thermal benefit for photovoltaic module thermal management, *ACS Photonics* 5 (2018) 1528–1538.
- [29] B. Zhao, M. Hu, X. Ao, G. Pei, Conceptual development of a building-integrated photovoltaic-radiative cooling system and preliminary performance analysis in Eastern China, *Appl. Energy* 205 (2017) 626–634.
- [30] E. Lee, T. Luo, Black body-like radiative cooling for flexible thin-film solar cells, *Sol. Energy Mater. Sol. Cell.* 194 (2019) 222–228.
- [31] Y. Lu, Z. Chen, L. Ai, X. Zhang, J. Zhang, J. Li, W. Wang, R. Tan, N. Dai, W. Song, A universal route to realize radiative cooling and light management in photovoltaic modules, *Solar RRL* 1 (2017).
- [32] Z. Cheng, H. Han, F. Wang, Y. Yan, X. Shi, H. Liang, X. Zhang, Y. Shuai, Efficient radiative cooling coating with biomimetic human skin wrinkle structure, *Nano Energy* 89 (2021).
- [33] B. Zhao, M. Hu, X. Ao, Q. Xuan, G. Pei, Spectrally selective approaches for passive cooling of solar cells: a review, *Appl. Energy* 262 (2020).
- [34] P. Bermel, M.M. Al-Jassim, X. Jin, P. Bermel, M.A. Alam, X. Sun, Y. Sun, Z. Zhou, *Thermal Radiation Management for Energy Applications*, 2017.
- [35] M. Strojnik, Z. Zhou, X. Sun, P. Bermel, *Infrared Remote Sensing and Instrumentation XXIV*, 2016.
- [36] X. Sun, T.J. Silverman, Z. Zhou, M.R. Khan, P. Bermel, M.A. Alam, Optics-based approach to thermal management of photovoltaics: selective-spectral and radiative cooling, *IEEE J. Photovoltaics* 7 (2017) 566–574.
- [37] J.N. Munday, T. Safi, Radiative Cooling of a GaAs Solar Cell to Improve Power Conversion Efficiency, *Ieee Phot Spec Conf*, 2016, pp. 1125–U1900.
- [38] Z. Zhou, Z. Wang, P. Bermel, Radiative cooling for low-bandgap photovoltaics under concentrated sunlight, *Opt Express* 27 (2019) A404–A418.
- [39] J.-W. Cho, S.-J. Park, S.-J. Park, Y.-B. Kim, K.-Y. Kim, D. Bae, S.-K. Kim, Scalable on-chip radiative coolers for concentrated solar energy devices, *ACS Photonics* 7 (2020) 2748–2755.
- [40] Z. Wang, D. Kortge, J. Zhu, Z.G. Zhou, H. Torsina, C. Lee, P. Bermel, Lightweight, passive radiative cooling to enhance concentrating photovoltaics, *Joule* 4 (2020) 2702–2717.
- [41] T.S. Safi, J.N. Munday, Improving photovoltaic performance through radiative cooling in both terrestrial and extraterrestrial environments, *Opt Express* 23 (2015) A1120–A1128.
- [42] X.S. Sun, R. Dubey, S. Chattopadhyay, M.R. Khan, R.V. Chavali, T.J. Silverman, A. Kottantharayil, J. Vasi, M.A. Alam, A novel approach to thermal design of solar modules: selective-spectral and radiative cooling, *IEEE Phot. Spec. Conf.* (2016) 3584–3586.
- [43] W. Li, Y. Shi, K. Chen, L. Zhu, S. Fan, A comprehensive photonic approach for solar cell cooling, *ACS Photonics* 4 (2017) 774–782.
- [44] B. Zhao, M. Hu, X. Ao, Q. Xuan, G. Pei, Comprehensive photonic approach for diurnal photovoltaic and nocturnal radiative cooling, *Sol. Energy Mater. Sol. Cell.* 178 (2018) 266–272.
- [45] Y. An, C. Sheng, X. Li, Radiative cooling of solar cells: opto-electro-thermal physics and modeling, *Nanoscale* 11 (2019) 17073–17083.
- [46] L. Zhou, H. Song, J. Liang, M. Singer, M. Zhou, E. Stegenburgs, N. Zhang, C. Xu, T. Ng, Z. Yu, B. Ooi, Q. Gan, A polydimethylsiloxane-coated metal structure for all-day radiative cooling, *Nat. Sustain.* 2 (2019) 718–724.
- [47] Y. Zhai, Y. Ma, S.N. David, D. Zhao, R. Lou, G. Tan, R. Yang, X. Yin, Scalable-manufactured randomized glass-polymer hybrid metamaterial for daytime radiative cooling, *Science* 355 (2017) 1062–1066.
- [48] G. Park, K. Roh, H. Kim, S. Khan, M. Lee, B.W. Kim, W. Kim, Universal experimental methods for evaluating the performance of radiative cooling materials, *Adv. Mater. Technol.* 7 (2021).
- [49] L. Qiu, Y. Ouyang, Y. Feng, X. Zhang, Review on micro/nano phase change materials for solar thermal applications, *Renew. Energy* 140 (2019) 513–538.
- [50] L. Qiu, Y. Ouyang, Y. Feng, X. Zhang, X. Wang, J. Wu, Thermal barrier effect from internal pore channels on thickened aluminum nanofilm, *Int. J. Therm. Sci.* 162 (2021).
- [51] A. Hasan, S.J. McCormack, M.J. Huang, B. Norton, Evaluation of phase change materials for thermal regulation enhancement of building integrated photovoltaics, *Sol. Energy* 84 (2010) 1601–1612.
- [52] S.A. Nada, D.H. El-Nagar, H.M.S. Hussein, Improving the thermal regulation and efficiency enhancement of PCM-integrated PV modules using nano particles, *Energy Convers. Manag.* 166 (2018) 735–743.
- [53] F. Selimefendigil, F. Bayrak, H.F. Oztop, Experimental analysis and dynamic modeling of a photovoltaic module with porous fins, *Renew. Energy* 125 (2018) 193–205.
- [54] K. Wang, G. Luo, X. Guo, S. Li, Z. Liu, C. Yang, Radiative cooling of commercial silicon solar cells using a pyramid-textured PDMS film, *Sol. Energy* 225 (2021) 245–251.
- [55] K. Gao, H. Shen, Y. Liu, Q. Zhao, Y. Li, J. Liu, Random inverted pyramid textured polydimethylsiloxane radiative cooling emitter for the heat dissipation of silicon solar cells, *Sol. Energy* 236 (2022) 703–711.
- [56] A.P. Raman, M.A. Anoma, L. Zhu, E. Rephaeli, S. Fan, Passive radiative cooling below ambient air temperature under direct sunlight, *Nature* 515 (2014) 540–544.
- [57] Modtran. http://modtran.spectral.com/modtran_home#plot, 2019. (Accessed 1 April 2019).